A Biometric Attack Case based on Signature Synthesis

Miguel A. Ferrer
Instituto Universitario para el Desarrollo Tecnológico y la Innovación en Comunicaciones
Universidad de Las Palmas de Gran Canaria, Spain
miguelangel.ferrer@ulpgc.es

Moises Diaz
Universidad del Atlantico Medio
Las Palmas de Gran Canaria, Spain
mdiazc@unidam.es

Cristina Carmona-Duarte
Instituto Universitario para el Desarrollo Tecnológico y la Innovación en Comunicaciones
Universidad de Las Palmas de Gran Canaria, Spain
criscarmonad@gmail.es

Réjean Plamondon
École Polytechnique,
Université de Montréal,
Montréal, P.Q., Canada.
rejean.plamondon@polymtl.ca

***Abstract*—One of the biggest challenges in on-line signature verification is the detection of malicious and skilled attacks. This paper proposes a new conceivable attack for an on-line signature biometric scheme. The attack consists in interpolating a smoothed 8-connected version of the forged signature and selecting the most relevant salient points, skipping those that belong to tremor or indecisive movements due to the faking procedure. The Sigma-Lognormal model is then used to synthetize the new on-line signature in the hope of obtaining an improved imitation. The experiments aim to prove that the False Acceptance Ratio (FAR) is significantly worsened with the Biosecure-SONOFF public on-line signature database. These results are expected to elicit new automatic signature verifiers able to cope with this new kind of attack.**

Keywords— Biometric attack, Synthetic signatures, Automatic Signature Verification, Sigma-Lognormal Model, Skillfully Skilled Forgeries

I. Introduction

Biometric systems are extensively used to identify people in legal and administrative tasks [1]. They are usually referred to as Pattern Identification systems, in which physiological or behavioral traits from a person are registered during the enrollment stage and stored as templates in a database for future comparisons [2]

The accuracy and reliability of these systems have decisive security implications. Indeed, the detection of forged signatures and the development of countermeasures have attracted the interest of academia and industry during the last decades [1]. However, these systems are subject to attacks in any of their stages.

In the case of on-line signature-based biometric systems, an attack can be performed on the input sensor, the feature extractor, the matcher, the decision maker or the database. The attack can be directed at any one of these components or any communication between them.

Recent technological developments have improved the capabilities of sensor devices, and they can be seen in the growth of tablets, phablets or smart phones such as the Wacom Intuos, Cintiq or iPads among others. Nevertheless, their computational and algorithmic capabilities have brought some downsides in security issues which increase the possibilities of biometric attacks at the sensor level. In fact, it is possible to introduce a program that modifies the input signature to delude the verifier. This paper focuses on the proposal of an attack to be implemented in a smart sensor for on-line signature verification.

Our study specifically looks at a conceivable novel attack at the sensor level, which consists in modifying a counterfeited signature in the hope of building up a more plausible genuine sample.

Some hypotheses are from neuroscience are borrowed in order to design dexterously skilled forgery signatures. The kinematic theory of rapid human movements and its associated Sigma-Lognormal model [3] are used for this purpose. This theory essentially models the velocity profile of a rapid movement, like a signature, as a weighted vector sum of delayed lognormals. Each of these lognormals represents a stroke. The overlapping of these lognormals can produce a complex trajectory from a hidden trajectory action plan. Such an action plan consists of a sequence of virtual target points linked together by circular arcs. Each arc is produced as a response of the motor system to a set of rhythmic commands from the cerebellum. The overlapping of these circular arcs along time result in a complex movement. One of the advantages of this model is that it considers physical body features such as the neuromuscular system response to the production of a signature.

It is possible to find in the literature applications of the Sigma-Lognormal model to model signatures. For example, in [4] the lognormal parameters are combined with classical parameters to improve a signature-based biometric system. They are also used to generate duplicated signatures to improve the training [5] or the improvement of forgery detection [6]. It has also been used to synthesize Western [7][8][9][10] and Indian [11][12] signatures.

The Sigma-Lognormal model has been used in the area of security and specifically in [13] to synthesize more skillful on-line forgeries. It allows more challenging data sets to be generated for training and testing purposes. In this study, the improved forgeries are produced by replacing their velocity profile with others closer to a genuine signature. It is carried out by fitting a sum of lognormals to the trajectory and resampling the trajectory with the new synthetic velocity profile. As a

978-1-5386-7931-9/18/$31.00 ©2018 IEEE

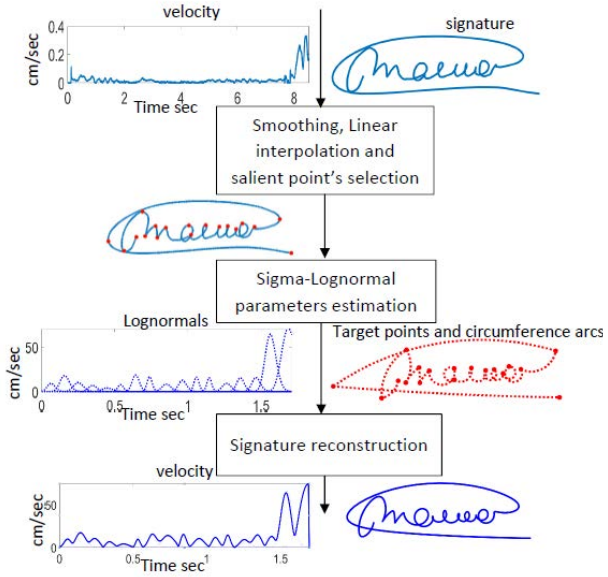

Figure 1. Procedure to reconstruct a genuine-like signature from a forgery.

result, the obtained velocity profile looks more genuine but the trajectory remains unchanged. That is, the trajectory keeps the characteristic doubtful trajectory of a forgery.

Our procedure is a step further from [13]. In this paper, if a skilled forgery is rejected by the system, the rejected signature is smoothed and linearly interpolated. The salient points of the signature are estimated along with their associated virtual target points. At this point, time stamps are assigned to the salient points, the Sigma-Lognormal parameters are calculated and the signature is reconstructed. This procedure is summarized in Figure 1.

The outline of the paper is as follows: Section 2 describes the basis of the Sigma-Lognormal model. Section 3 is dedicated to the salient point's estimation while Section 4 develops the signature reconstruction procedure. The experimental results are given in Section 5 while Section 6 closes the paper with conclusions and discussion.

II. SigmaLognormal Model

The new signature is obtained from the Kinematic theory of rapid movements. It claims that a human being performs its movements as an overlapped sum of N strokes in which the velocity profile $v_j(t)$ of the j^{th} stroke can be modeled as a lognormal [3]:

$$v_j\left(t; t_{0_j}, \mu_j, \sigma_j^2\right) = D_j \Lambda\left(t; t_{0_j}, \mu_j, \sigma_j^2\right) = \\ = \frac{D_j}{\sigma_j \sqrt{2\pi}(t - t_{0_j})} exp\left\{-\frac{\left[ln\left(t - t_{0_j}\right) - \mu_j\right]^2}{2\sigma_j^2}\right\} \quad (1)$$

where t is time, t_{0_j} the time of stroke command occurrence, D_j the amplitude of the stroke, μ_j the stroke delay and σ_j the stroke response time, both on a logarithmic time scale.

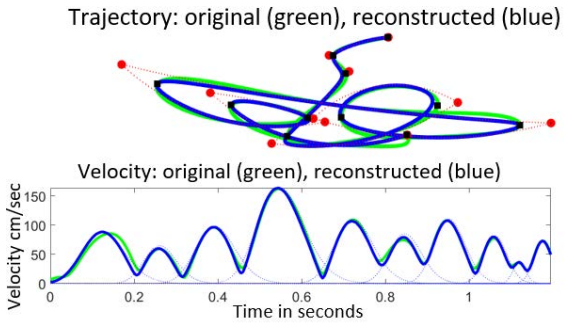

Figure 2. Results of the trajectory and velocity representation with the Sigma-Lognormal model. Upper. Trajectory: original (green), reconstructed (blue), Virtual Target Points (red circles), arcs between target points (red dotted) and Salient Points (black squares). Down. Velocity: original (green), reconstructed (blue) and lognormals (dotted blue)

The overlapping of these lognormals can produce a complex trajectory from a hidden trajectory action plan. Such an action plan consists of a sequence of virtual target points linked together by circular arcs. Each arc is produced as a response of the motor system to a set of rhythmic commands from the cerebellum. The overlapping of these movements, in time, results as:

$$\vec{v}(t) = \begin{bmatrix} v_x(t) \\ v_y(t) \end{bmatrix} = \sum_{j=1}^{N} D_j \begin{bmatrix} cos\phi_j(t) \\ sin\phi_j(t) \end{bmatrix} D_j \Lambda\left(t; t_{0_j}, \mu_j, \sigma_j^2\right) \quad (2)$$

where N is the number of lognormal strokes and $\phi_j(t)$ is the angular position.

$$\phi_j(t) = \theta_{s_j} + \frac{\theta_{e_j} - \theta_{s_j}}{2}\left[1 + erf\left(\frac{ln\left(t - t_{0_j}\right) - \mu_j}{\sigma_j \sqrt{2}}\right)\right] \quad (3)$$

θ_{ej} and θ_{sj} being the starting angle and the ending angle of the arc that links the two virtual target points that belong to the j^{th} stroke. Note that this formula describes the sweeping from θ_{s_j} to θ_{e_j} in a lognormal timing. Finally, the trajectory is worked out as:

$$\vec{s}(t) = \begin{bmatrix} x_r(t) \\ y_r(t) \end{bmatrix} = \sum_{j=1}^{N} \frac{D_j}{\theta_{e_j} - \theta_{s_j}} \begin{bmatrix} sin\phi_j(t) - sin\theta_{s_j} \\ -cos\phi_j(t) + cos\theta_{s_j} \end{bmatrix} \quad (4)$$

This formula converts angles into circular arcs and overlaps them. Specifically, the j^{th} term of the summation represents the arc of the circumference that links the virtual target points tp_{j-1} and tp_j. The radius of such circumference is $D_j / \left(\theta_{e_j} - \theta_{s_j}\right)$ and D_j represents the arc length. In this case, the virtual target points are defined by:

$$tp_j = tp_{j-1} + \frac{D_j}{\theta_{e_j} - \theta_{s_j}} \begin{bmatrix} sin\phi_j(T) - sin\theta_{s_j} \\ -cos\phi_j(T) + cos\theta_{s_j} \end{bmatrix} \quad (5)$$

T being the duration or the temporal length of the signature.

An example of an original signature, the reconstruction of its trajectory as sum of circular arcs between virtual target points and the velocity reconstruction as the sum of lognormals is shown in Figure 2.

III. SALIENT POINTS ESTIMATION

This section works out the salient points in the signature trajectory. Bear in mind that the reconstructed signature is sensitive to the accurate selection of the salient points. Indeed, it is the initial step of the proposed procedure to synthetize a genuine-like signature from a forgery. The first step smooths the forgery's trajectory in order to reduce the possible tremor in the trajectory. The second step estimates the salient points focusing on the most relevant corners and skipping those likely provoked by the faking procedure.

A. Trajectory Smoothing

The tremor is reduced in two steps. The first one interpolates the trajectory at 200Hz using cubic splines. The second step applies a low pass filter. Specifically, we use a linear phase FIR filter with cutting frequency at 16Hz. This smoothing also helps to avoid a false salient point due to a tremor in indecisive trajectories which are usually seen in a forgery's trajectory.

B. Estimation of the salient points

The salient points correspond to zones with high curvature. These points usually represent a minimum in the velocity profile. Note that we are not interested in the salient points of the forgery but in the salient points of the signature eventually written by the genuine users. That is, we attempt to avoid the salient point due to a tremor or indecision. For this reason, a multiresolution salient point's estimator has been used [14] [15] which defines the curvature of each point at different scales.

The procedure is as follows. The samples of the smoothed signature are linearly 8-connected obtaining the trajectory of M samples: $\{x_o[n], y_o[n]\}_{n=1}^{M}$.

Then, for each scale T, a distance between samples is described as $d(T) = \text{round}(M/(T-1)), T = 3, \dots, M$. The curvature $\alpha_T(n)$ at point $(x_o[n], y_o[n])$ is worked out as the angle formed by the two segments, which connect $(x_o[n], y_o[n])$ with $(x_o[n-d(T)], y_o[n-d(T)])$ and $(x_o[n+d(T)], y_o[n+T])$. Then, a matrix $A(i,j) = \alpha_{i+2}(j)$ of $M-2$ rows and M columns is built up.

Once the curvature matrix has been worked out, we estimate the curvature along the trajectory as $C(l) = \sum_{i=1}^{M-2} A(i,l) / (M-2)$. The salient points are selected as the peaks whose height/width ratio are greater than $(max(C) - \min(C))/45$ and are separated by more than 1/10 the width of the signature. A velocity profile quite similar to a genuine signature is guaranteed, which is generally quick and swift. In this way, we work out the N salient points $sp_j, j = 0, \dots, N$, where sp_0 and sp_N are the first and the last sample of the trajectory, respectively.

A drawback to this approach is that this step is computationally very demanding. However, from a practical point of view, all the scales $T = 3 \dots M$ are not required. In fact, the lower scales are too coarse for a feasible detection of the corners. Therefore, a dozen scales uniformly distributed between $T = M/2$ and $T = M$ have been used to speed up the first step

A visual example is shown in Figure 2. A further description of this procedure can be found in [14].

IV. SIGNATURE RECOSTRUCTION

The signature is reconstructed form the skilled forgery trajectory and its selected salient points. It is carried out following the Sigma-Lognormal model. Therefore, the signature is analytically represented as a sum of N strokes and defined with their parameters, which are D_j, $t_{0_j}, \mu_j, \sigma_j^2, tp_j$, $\theta_{s,j}$ and $\theta_{e,j}, \forall j = 1, \dots, N$.

A. Stroke Segmentation

The limits of the strokes are defined by the salient point. The occurrence time of each salient point t_{min_j} is computed from the so-called Central Pattern Generators (CPG) that produces rhythmic patterned outputs, without sensory feedback, to activate different motor pools [16]. This can be observed in the clearly periodic pattern of the handwriting velocity. Therefore, if the stroke generation is assimilated into the CPG step cycle, the duration of each stroke can be very similar with a value around 0.1 seconds. This hypothesis lead us to define $t_{min_j} = 0.1 \times j$ sec.

B. Velocity profile synthesis

In this section, a lognormal is fitted in with each stroke. Let us assume a single stroke velocity profile given by $v_j(t)$. The values of D_j, μ_j and σ_j^2 are set from the following two hypotheses: Firstly, the margins for natural human handwriting given in [3]. Secondly, it was heuristically observed that most of the lognormals are centered when the Biosecure-SONOFF is represented by using ScriptStudio [2], i.e. the lognormal peaks approach the center of the strokes. Therefore, we configure our skewness close to zero but positive and the kurtosis around 3.

The calculation of these values is suggested as follows. From Eq. 1, the distance $s(t)$ traveled at time t is obtained as:

$$s(t) = \int_{-\infty}^{\infty} v_j(t)dt = \frac{D_j}{2}\left(1 + \text{erf}\left(\frac{\ln\left(t - t_{0_j}\right) - \mu_j}{\sqrt{2}\sigma_j}\right)\right) \quad (6)$$

Then, let l_s be the length of a stroke, i.e. the length of the arc between two consecutive minima. From Eq. (6) we deduce:

$$l_s = \frac{D_j}{2}\left(1 + \text{erf}\left(\frac{\ln\left(t - t_{0_j}\right) - \mu_j}{\sqrt{2}\sigma_j}\right)\right) \quad (7)$$

As $\text{erf}(3) \to 1$, a possible solution of Eq. (7) is:

$$D_j = l_s \quad (8)$$

$$\mu_j = \ln\left(t - t_{0_j}\right) - 3\sqrt{2}\sigma_j \quad (9)$$

Furthermore, as the lognormals are centered in the middle of the stroke with a low positive skew, their maximum or mode, defined by $e^{\mu_j - \sigma_j^2}$, is around $t_{max_j} = t_{min_{j-1}} + 0.05$ with a slightly left skew. Therefore, it holds that:

$$t_{max_j} - t_{0_j} = e^{\mu_j - \sigma_j^2} \quad (10)$$

Combining Eq. (9) and Eq. (10) we obtain:

$$\sigma_j^2 + 3\sqrt{2}\sigma_j - \ln k = 0 \quad (11)$$

Thus, in the case of an isolated stroke of length l_s and duration 0.1 sec, the simplified approach leads us to estimate σ_j^2 as the positive solution of the simple second order equation

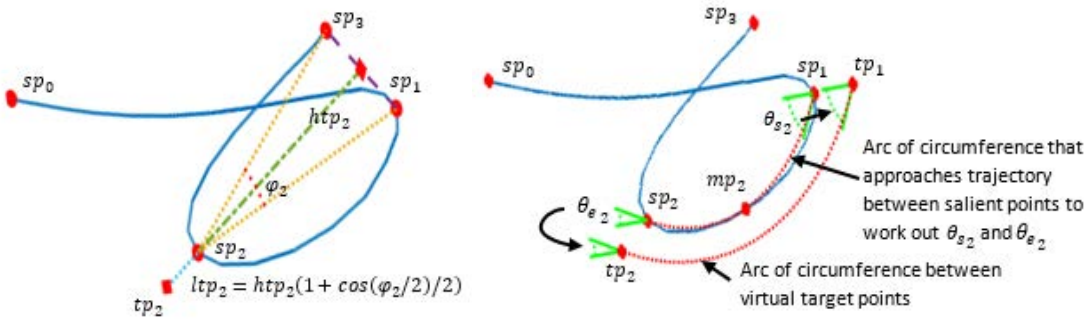

Fig. 3. Left: Estimation of the target point tp_2 from salient points sp_1, sp_2, and sp_3. Right: Estimation of values θ_{s_2} and θ_{e_2} for the second stroke

Eq.(11), and μ_j by substituting σ_j^2 in Eq. (10). The value D_j is worked out later as we do not know l_s yet.

Regarding t_{0_j}, it is well-known that the movement action motion is issued in the cortex. It then passes through the Basal Ganglia, which decodes the message in order to activate the different pool of muscles to carry out such movement. In a well-learned movement, it is reasonable to assume that the time between the movement action is issued and the performed movement should be rather similar for each stroke. In our procedure, this tramission time is approched by $t_{min,j-1} - t_{0_j}$ which is known to be around 0.3 seconds [17]. Speciffically, in our case, $t_{0_j} = t_{min,j-1} - 0.3$.

C. Location of the Initial Virtual Target Points tp_j

Given that the virtual target points refers to spatial trajectory, these points are directly estimated from the original trajectory. Each salient point sp_j is associated to a virtual target point tp_j, $j = 0, \dots, N$. Specifically, $tp_0 = sp_0$ and $tp_N = sp_N$ which are the first and last point of the trajectory. This way, the virtual target point tp_j, $\forall j = 1, \dots, N-1$, is calculated using sp_{j-1}, sp_j and sp_{j+1}, which form a triangle. The initial virtual target point is located on the median of the vertex sp_j, which is a straight line through the vertex sp_j and the midpoint $(sp_{j-1} + sp_{j+1})/2$ of the opposite side, at a distance ltp_j from the vertex sp_j, defined as:

$$ltp_j = htp_j cos(\varphi_j/2) \quad (12)$$

where htp_j is the distance between the vertex sp_j and the midpoint of the opposite side and φ_j is the angle of the vertex sp_j. Applying the cosine function we see that the closer angles of the vertex sp_j produce greater distances of tp_j from sp_j. An example of this procedure is shown on the left hand side of Figure 3.

D. Estimation of Initial θ_{s_j} and θ_{e_j}

The angles of the circumferences that link virtual target points are defined with their start θ_{s_j} and end θ_{e_j} angles for $j = 1, \dots, N$ where N is the total number of strokes. The spatial characteristic of the signature requires that the estimates use the original spatial trajectory.

They are calculated as follows:

1. The middle point mp_j of the trajectory of the j^{th} stroke between the salient points sp_{j-1} and sp_j is worked out. Middle point in this context means the same distance on the trajectory from mp_j to sp_{j-1} and sp_j.
2. A circumference that passes by these three points is obtained.
3. The angle θ_{s_j} is computed as the angle of the tangent of the circumference in sp_{j-1}. Then, the angle θ_{e_j} is obtained as the angle of the tangent of the circumference in sp_j.

An illustration of this procedure is shown on the right hand side of Figure 3.

E. Reconstructed Spatial Trajectory

The above procedure produces an estimation of the parameters of the Sigma-Lognormal model $t_{0_j}, \mu_j, \sigma_j^2, \theta_{s_j}$ and $\theta_{e_j}, \forall j = 1, \dots, N$ and $tp_j, \forall j = 0, \dots, N$, from the original salient points $sp_j, \forall j = 0, \dots, N$ and observed samples $\{x_o(t), y_o(t)\}$, in the range $0 < t < T$. These parameters are used to calculate the parameters D_j and reconstruct the signature $T_r(t) = \{x_r(t), y_r(t)\}$, following equations (3) and (4). $T_r(t)$ is the trajectory obtained from the skilled forgery that imitates a genuine one.

1) Estimation of D_j

The value of the lognormal amplitude D_j describes the amplitude of the movement and is defined without ambiguity by the position of the virtual target points tp_{j-1}, tp_j, $\theta_{s,j}$ and $\theta_{e,j}$. It is calculated as:

$$D_j = r_j\left(\theta_{e_j} - \theta_{s_j}\right), \quad j \in 1, \dots N \quad (13)$$

where r_j is the radius of the circunference that goes from tp_{j-1} to tp_j. To work out r_j, we first calculate the center of the circumference as the intersection of the line that transverses tp_{j-1} with slope $-1/\tan\theta_{s_j}$ and the line that transvverses tp_j with slope $-1/\tan\theta_{e_j}$.Then, r_j is the distance from the center of the circumference to either tp_{j-1} or tp_j.

An example of a recovered spatial trajectory is shown in Figure 4. Note that the execution time has been reduced by two meaning that the signature has been written quicker and swifter.

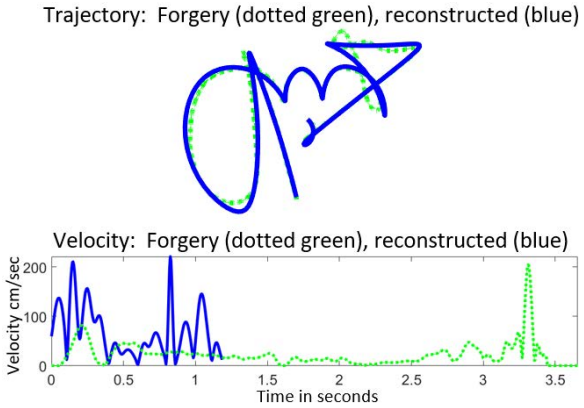

Figure 4.Original and reconstructed skilled forgery trajectory (upper) and velocity (below).

Furthermore, the trajectory is more rounded even in the areas where the original forgery reveals more doubts uncertainty or indecision. Therefore, it is expected that the reconstruted signature will be seen more genuine-like than the original forgery by the classifier

V. Experiments

The experiments are aimed to verify whether the reconstructed signatures are more genuine-like than the original forgeries, using the following steps: 1) The performance of an on-line signature database is worked out for skilled forgeries by using two on-line ASV; 2) The skilled forgeries are reconstructed and 3) The performance of the database with the reconstructed skilled forgeries is worked out and compared with the original skilled forgeries. In this way we can study the reach of the improved biometric attack for on-line signature ASV.

A. Database

The experiments have been carried out with the publicly available database called Biosecure-SONOFF, that comprises both on-line and off-line signatures. The signatures were simultaneously acquired by fixing a sheet over a Wacom Intuos3 A4/Inking pen tablet. Each donor was asked to sign on the paper his inked signature with the inked tablet pen. After registering the on-line signature, the paper sheet was scanned and the signature image saved with the same codename. It was recorded through 4 sessions spanning 4 months, each session contains 4 genuine signatures and 3 forgeries. In total 132 users, 16 genuine and 12 forgeries [18].

B. Comparing False Acceptance and Rejection Rate curves

We compare the False Acceptance Rate (FAR) and False Rejection Rate (FRR) curves of both original skilled forgeries and reconstructed signatures from skilled forgeries. The evaluation considers two state-of-the-art on-line ASV: a Dynamic Time Warping (DTW) [19] and an own implementation of the Manhattan-based distance ASV [20].

Both ASVs were trained with the first 5 genuine signatures of the Biosecure-SONOFF database. For FRR, we used the remaining 11 genuine signatures of the same signer. The FAR

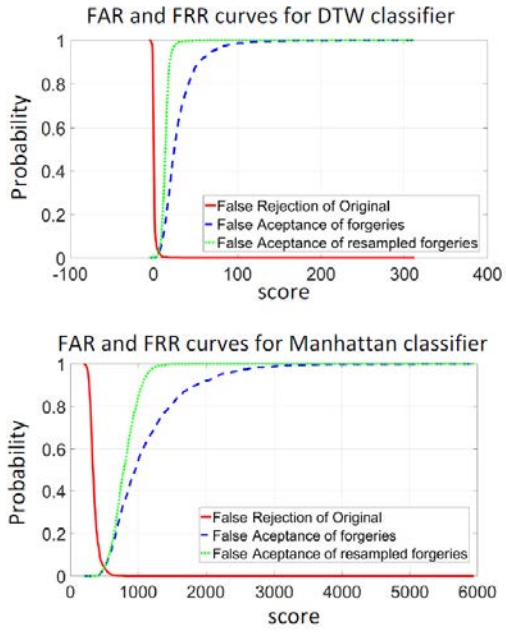

Figure 5. FAR and FRR curves for genuine, forgery and reconstructed signatures.

curves were calculated using the 12 available skilled forgeries of each signer.

The resulting FAR and FRR curves are shown in Figure 5. Notice that the FAR curve of the reconstructed skilled forgeries is closer to the FRR curve than the FRR of the original skilled forgeries. The same effect is observed on both classifiers. This means that the reconstructed skilled forgeries are closer to the genuine signature than the forgeries. Therefore, it can be seen that the proposed procedure produces improved forgeries that are more difficult to detect.

Table I and II also compare the exact rates of the FRR for forgeries and reconstructed forgeries at certain FAR rates. In this table, it is possible to appreciate the deterioration of the ASV when using this kind of biometric attack. In the case of the DTW, for a given FRR around the EER, the results worsen by around 65% which means that the FRR is multiplied by 1.7. In the case of the classifier based on the Manhattan distance, the deterioration is less, around 7% on average. Nevertheless, both ASV show that better improvements are obtained when FRR is reduced.

VI. Conclusion

This paper proposes a biometric attack case study for on-line signature verification. The attack consists in generating an improved imitation from a forgery.

While a well-trained forger can accurately imitate the genuine signature trajectory, they usually fail to feasibly emulate the velocity profile. Therefore, a way to generate an improved imitation would be to reconstruct the forgery with a genuine-like velocity profile and a smoother trajectory.

The new improved forgeries are generated using the kinematic theory of rapid movements and its associated Sigma-

TABLE I. FAR AND FRR WITH DTW-BASED ASV

GENUINE	FORGERIES	RECONSTRUCTED	DETERIORATION
FRR	FAR	FAR	
0,0252	0,017	0,0284	67,06%
0,022	0,0227	0,0366	61,23%
0,0189	0,0309	0,0505	63,43%
0,0157	0,0429	0,0657	53,15%
0,0126	0,0455	0,0751	65,05%
0,0094	0,0537	0,0997	85,66%
0,0063	0,0568	0,1155	103,35%
0,0031	0,0814	0,1926	136,61%
0	0,6585	0,9931	50,81%

TABLE II. FAR AND FRR WITH MANHATTAN-BASED ASV

GENUINE	FORGERIES	RECONSTRUCTED	DETERIORATION
FRR	FAR	FAR	
0,0452	0,036	0,0372	3,33%
0,0395	0,0391	0,0398	1,79%
0,0339	0,0467	0,048	2,78%
0,0282	0,0549	0,0587	6,92%
0,0226	0,0631	0,0682	8,08%
0,0169	0,077	0,0846	9,87%
0,0113	0,0979	0,1124	14,81%
0,0056	0,1225	0,1427	16,49%
0	0,3535	0,5246	48,4%

Lognormal model.

The procedure smooths the forgery's trajectory to avoid tremor and indecisive trajectories and selects salient points related with a genuine handwritten signature. The salient points are then used to obtain the virtual target points from which the Sigma-Lognormal model parameters are calculated. The timeline is generated using the hypothesis of a periodic pattern of the handwriting velocity with a period around 0.1 second.

The experiments show the success of the biometric attack by analyzing the improvement in the FAR curve for any point in the FRR curve. These experiments were conducted with two conceptually different on-line ASV in order to measure the generalization of the biometric attack. As a result, it is shown that this procedure is more effective with classifiers based on alignment such as DTW than with a classifier based on a histogram of distances such as the Manhattan one.

Some further work is still required to improve the reconstruction, mainly in the selection of the target points. As future research, a reliable and accurate way of detecting such reconstructed signatures would be an essential countermeasure.

ACKNOWLEDGMENT

This study was funded by the Spanish government's MIMECO TEC2016-77791-C4-1-R research project and European Union FEDER program/funds. C. Carmona-Duarte is supported by a Juan de la Cierva grant (IJCI-2016-27682) from the Spanish MINECO and NSERC grant RGPIN-2015-06409 supported R. Plamondon.

REFERENCES

[1] D. Impedovo and G. Pirlo, "Automatic Signature Verification: The State of the Art," *IEEE Trans. Syst. Man, Cybern. Part C (Applications Rev.*, vol. 38, no. 5, pp. 609–635, Sep. 2008.

[2] A. K. Jain, K. Nandakumar, and A. Ross, "50 years of biometric research: Accomplishments, challenges, and opportunities," *Pattern Recognit. Lett.*, vol. 79, pp. 80–105, Aug. 2016.

[3] C. O'Reilly and R. Plamondon, "Development of a Sigma-Lognormal representation for on-line signatures," *Pattern Recognit.*, vol. 42, no. 12, pp. 3324–3337, 2009.

[4] A. Fischer, R. Plamondon, "Signature Verification Based on the Kinematic Theory of Rapid Human Movements," *IEEE Trans. Human-Machine Syst.*, vol. 47, no. 2, pp. 169–180, Apr. 2017.

[5] M. Diaz, A. Fischer, M. A. Ferrer, and R. Plamondon, "Dynamic Signature Verification System Based on One Real Signature," *IEEE Trans. Cybern.*, vol. 48, no. 1, pp. 228–239, Jan. 2018.

[6] M. Gomez-Barrero, J. Galbally, J. Fierrez, J. Ortega-Garcia, and R. Plamondon, "Enhanced on-line signature verification based on skilled forgery detection using Sigma-LogNormal Features," in *2015 International Conference on Biometrics (ICB)*, 2015, pp. 501–506.

[7] J. Galbally, R. Plamondon, J. Fierrez, and J. Ortega-Garcia, "Synthetic on-line signature generation. Part I: Methodology and algorithms," *Pattern Recognit.*, vol. 45, no. 7, pp. 2610–2621, Jul. 2012.

[8] J. Galbally, J. Fierrez, J. Ortega-Garcia, and R. Plamondon, "Synthetic on-line signature generation. Part II: Experimental validation," *Pattern Recognit.*, vol. 45, no. 7, pp. 2622–2632, Jul. 2012.

[9] M. A. Ferrer, M. Diaz-Cabrera, and A. Morales, "Static Signature Synthesis: A Neuromotor Inspired Approach for Biometrics," *IEEE Trans. Pattern Anal. Mach. Intell.*, vol. 37, no. 3, pp. 667–680, Mar. 2015.

[10] M. A. Ferrer, M. Diaz, C. Carmona-Duarte, and A. Morales, "A Behavioral Handwriting Model for Static and Dynamic Signature Synthesis," *IEEE Trans. Pattern Anal. Mach. Intell.*, vol. 39, no. 6, 2017.

[11] M. Diaz *et al.*, "Multiple Generation of Bengali Static Signatures". 15th International Conference on Frontiers in Handwriting Recognition (ICFHR), Shenzhen, China, 23-26 October 2016, pp. 42-47.

[12] M. A. Ferrer *et al.*, "Static and Dynamic Synthesis of Bengali and Devanagari Signatures," *IEEE Trans. on. Cybernetics*, pp. 1–12, 2018.

[13] M. Ferrer, M. Diaz, C. Carmona-Duarte, and R. Plamondon, "Improving on-line signature skillfulness," in *Workshop on Lognormality Principle and its Applications in Int. Conf. on Pattern Recognition and Artificial Intelligence, ICPRAI 2018*, Montreal, Canada, 14-17 May 2018, pp 768-773.

[14] M. A. Ferrer, M. Diaz, C. Carmona-Duarte, "Two-Steps Perceptual Important Points Estimator for Static Signature," in *Intl. Conference on Image Processing Theory, Tools @ Application*, 2017, pp. 1–6.

[15] C. De Stefano, M. Garruto, and A. Marcelli, "A saliency-based multiscale method for on-line cursive handwriting shape description," in *Proceedings - International Workshop on Frontiers in Handwriting Recognition, IWFHR*, 2004, pp. 124–129.

[16] G. Gandadhar, "A Neuromotor Model of Handwriting Generation: Highlighting the Role of Basal Ganglia," Thesis submitted at Departament of Electrical Engineering, Indian Institute of Technology, Madras, 2006.

[17] E. R. Kandel, J. H. Schwartz, and T. M. Jessell, *Principles of Neural Science*, vol. 4. 2013.

[18] J. Galbally, M. Diaz-Cabrera, M. A. Ferrer, M. Gomez-Barrero, A. Morales, and J. Fierrez, "On-line signature recognition through the combination of real dynamic data and synthetically generated static data," *Pattern Recognit.*, vol. 48, no. 9, pp. 2921–2934, Sep. 2015.

[19] A. Fischer, M. Diaz, R. Plamondon, and M. A. Ferrer, "Robust score normalization for DTW-based on-line signature verification," in *Proceedings of the International Conference on Document Analysis and Recognition, ICDAR*, 2015, vol. 2015–Novem, pp. 241–245.

[20] N. Sae-Bae, N. Memon, "Online Signature Verification on Mobile Devices," *IEEE Trans. Inf. Forensics Secur.*, vol. 9, no. 6, pp. 933–947, Jun. 2014.